Basic Concepts in Architectured Materials

Mater. Res. Soc. Symp. Proc. Vol. 1188 © 2009 Materials Research Society 1188-LL01-01

Mechanical Principles of a Self-Similar Hierarchical Structure

Huajian Gao
Division of Engineering, Brown University, Providence, RI, 02912, USA

ABSTRACT

Natural materials such as bone, shell, tendon and the attachment system of gecko exhibit multi-scale hierarchical structures. Here we summarize some recent studies on an idealized self-similar hierarchical model of bone and bone-like materials, and discuss mechanical principles of self-similar hierarchy, in particular to show how the characteristic length, aspect ratio and density at each hierarchical level can be selected to achieve flaw tolerance and superior stiffness and toughness across scale.
Tel.: (401) 863-2626; Email address: Huajian_Gao@Brown.edu

INTRODUCTION

Multi-level structural hierarchy can be observed in many biological systems including bone [1-6] and attachment pads of gecko [7-9]. In fact, structural hierarchy is a rule of nature. Hierarchical structures can be observed in all biosystems from chromosome, protein, cell, tissue, organism, to ecosystems. What are the roles and principles of structural hierarchy? What determine the size scales and other geometrical factors in a hierarchical material? These questions should be of general interest to both engineering and biological systems.

Recent studies on biological materials have shown that the characteristic size at each level of structural hierarchy may have been selected to ensure tolerance of material/structural flaws. For example, it has been demonstrated [10,11] that, due to their nanoscale characteristic size, the mineral bits in bone and bone-like materials tend to fail not by propagation of pre-existing cracks but by uniform rupture at the limiting strength of the material. For biological adhesion systems [7,8,12], similar transition from crack-like failure to uniform rupture has also been discussed [13]; the adhesion strength is affected not only by the size but also by the shape of the contacting surfaces: the smaller the size, the less important the shape, and shape-insensitive optimal adhesion was found to become possible when the structural size is reduced to below a critical length around 100 nm for van der Waals adhesion [14].

In this paper, we summarize some recent studies on an idealized self-similar hierarchical model mimicking the structure of bone [6,15]. It is known that bone and bone-like materials (Fig. 1) exhibit hierarchical structures over many length scales. For example, sea shells have 2 to 3 levels of lamellar structure [1,2,16-18], while vertebral bone has 7 levels of structural hierarchy [2, 19-22] (Fig. 2). Although the higher level structures of bone and bone-like materials show great complexity and variations, they exhibit a generic nanostructure (Fig. 2) at the most elementary level of structural hierarchy consisting of nanometer sized hard mineral

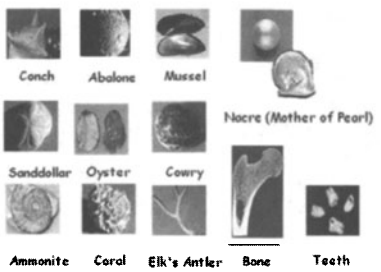

Figure 1. Bone and bone-like materials.

crystals arranged in a parallel staggered pattern in a soft protein matrix [3,5,10]. The nanostructure of tooth enamel shows needle-like (15–20nm thick and 1000nm long) crystals embedded in a relatively small volume fraction of a soft protein matrix [23-25]. The nanostructure of dentin and bone consists of plate-like (2–4nm thick and up to 100nm long) crystals embedded in a collagen-rich protein matrix [19,20], with the volume ratio of mineral to matrix on the order of 1 to 2. Nacre is made of very high volume fraction of plate-like crystals (200–500nm thick and a few micrometers long) with a small amount of soft matrix in between [1,2,16-18,26]. Bone and nacre are constructed with basically the same type of nanostructure made of staggered plate-like hard inclusions in a soft matrix. This staggered nanostructure is primarily subjected to uniaxial loading, as shown in Fig. 2.

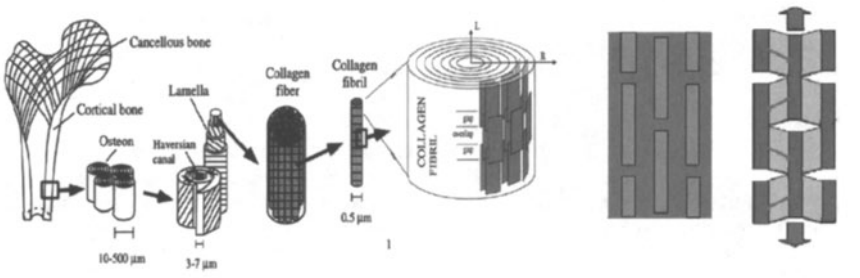

Figure 2. Hierarchical structures of bone and the generic nanostructure of bone-like materials [3, 10, 21].

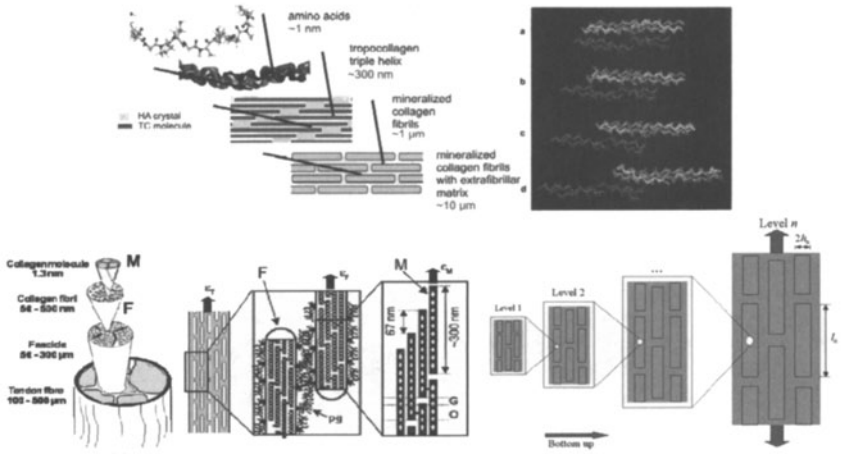

Figure 3. Self-similar structural hierarchy in bone and tendon [6,15,27,28].

As an example of hierarchical structures, in this paper we discuss an idealized hierarchical material with multiple levels of self-similar structures mimicking the staggered nanostructure of bone [6,15], as shown in Fig. 3. The resulting composite structure is still made of mineral and protein at some volume fraction, but the material is now distributed in a highly non-homogeneous way to form a hierarchical material with different properties at different length scales. In principle, this self-similar model can have arbitrary levels of hierarchy and at each level exhibits the same structure of slender hard plates arranged in a parallel staggered pattern in a soft matrix, similar to the nanostructure of bone. At each level of hierarchy, three mechanical principles will be required to determine three geometrical parameters: the width, length and volume fraction of hard inclusions.

MECHANICAL PRINCIPLES OF SELF-SIMILAR HIERARCHY

Principle I: Selection of characteristic length for uniform stress in hard particles at failure

Biological systems must be robust for survival. Therefore, the first principle of biocomposite is postulated to be that of flaw tolerance. Since the staggered biocomposite structure is primarily subjected to uniaxial tension, as shown in Fig. 2, the path of load transfer in the structure follows a tension-shear chain with the hard plates under tension and the soft matrix under shear. Analysis based on this tension-shear chain model [10, 29] showed that the integrity of biocomposites hinges upon the tensile strength of the hard particles. In order to keep the structure intact during deformation, the hard particles must be able to sustain large tensile load without fracture, while the protein/particle interface and the protein layer transfer load via shear and dissipate energy. The essence of flaw tolerance is to maximize the load carrying potential of the hard particles, which amounts to avoiding crack propagation until the material reaches its limiting strength. Theoretical estimation based on interatomic force laws shows that the theoretical strength is around $E/30$, where E is the Young's modulus. In reality, however, such high strength is rarely observed due to the inevitable presence of crack-like flaws which, under external loading, induce stress concentration near the tips of these flaws. As the external load reaches a critical value, the solid would fracture via crack propagation instead of simultaneous breaking of all bonds as assumed in the definition of *theoretical strength*. Under this circumstance, the load carrying capacity of the material is not utilized most efficiently since only a small fraction of material is maximally stressed at any instant of time during failure, leading to a

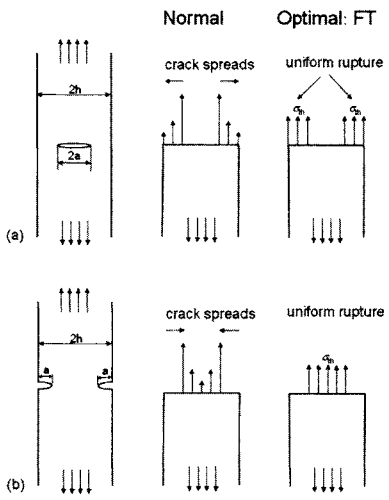

Figure 4. Illustration of flaw tolerance in a stretched strip particle with (a) a center crack or (b) two edge cracks. Under normal engineering circumstances, such cracked particle would fail by crack propagation at a critical applied load. However, as the strip width is reduced to below a critical value, the cracked particle would fail by uniform rupture near theoretical strength irrespective of the crack size. This state of material is termed flaw tolerance (FT).

much reduced "apparent" strength in contrast to the theoretical value. From the robustness point of view, an ideal scenario is to achieve the state of *flaw tolerance* [10,11] in which the material fails at the theoretical strength irrespective of the presence and size of cracks. Due to the random, unpredictable nature of crack-like flaws, it may seem at a first glance extremely difficult or impossible to eliminate stress concentration for large cracks so as to ensure uniform stress at material failure. However, theoretical arguments based on the well established concepts in fracture mechanics [6, 15] showed that this is actually possible with hierarchical material design.

The concept of uniform stress at failure can be demonstrated by a simple example involving an elastic strip particle containing a random internal or two edge cracks under tension (Fig. 4). Theoretical investigation of this problem based on the Dugdale cohesive model [11] showed that the cracked particle can indeed achieve uniform stress at failure for arbitrary crack size as long as the half-width h of the strip satisfies the following condition

$$h \le h_{cr} = \frac{\Gamma E}{S^2}, \tag{1}$$

where E is the Young's modulus, and S and Γ stand for the theoretical strength and fracture energy of the strip, respectively. For brittle materials, the fracture energy, which represents the amount of energy required for a unit increment of crack area, is usually taken to be twice of the surface energy, i.e., $\Gamma = 2\gamma$. Assuming no over-design of materials, we can just take the equality in Eq. (1) and write the condition of flaw tolerance as

$$\frac{\Gamma E}{S^2 h} = 1. \tag{2}$$

The principle of flaw tolerance thus yields a concrete equation to determine the characteristic dimension of the structure such that the stress in the structure is kept uniform even at the critical point of failure.

Principle II: Selection of aspect ratio for uniform stress in the matrix at failure

The next question is how the aspect ratio of the hard plates should be chosen. There have been two interesting considerations here. The first is to keep the stress in the matrix uniform up to failure. In a way, this is actually similar to Principle I. For this to happen, the length of the hard particle must not exceed a characteristic length defined as [30]

$$L_c = h\sqrt{\frac{2E\Theta_p(1-\varphi)}{\varphi\tau_p}} \tag{3}$$

where the subscript "p" stands for protein, τ_p is the shear yield strength of the protein matrix, Θ_p denotes the effective range of strain-to-failure of protein; φ denotes the volume fraction and E is the Young's modulus of hard particles. The concept of a characteristic length for stress transfer was first introduced via the classical shear lag model [31-33] and has played a key role in understanding mechanical properties of composites [34]. For a given length ℓ of hard particles, if we assume that the shear stress is equal to τ_p within the stress transfer zone and zero outside this zone at failure, we would expect that the maximum load transfer in the structure should satisfy the scaling law

$$\frac{P}{L_c \tau_p} = \begin{cases} \dfrac{\ell}{L_c} & \dfrac{\ell}{L_c} \le 1 \\ 1 & \dfrac{\ell}{L_c} \ge 1 \end{cases} \qquad (4)$$

Numerical simulations [30], as shown in Fig. 5, confirm that stress transfer in the staggered biocomposites is most efficient when the length of the hard particles is equal to the characteristic length L_c.

The second consideration is that, even when the shear stress in the matrix is uniform, as assumed in the tension-shear chain model, the aspect ratio of the particles could be further adjusted to ensure that the matrix, the particles and their interfaces reach their respective limiting strengths at the same time [6,10], i.e.

$$\tau_p = \tau_{\text{int}} = S / \rho \qquad (5)$$

Therefore, the aspect ratio of particles can be selected to ensure (1) that the stress in the matrix remains uniform even at the failure point and (2) that the soft matrix, the hard particles and their interfaces fail at the same time.

Similar concept of a characteristic length has been developed for optimal overlap length between two tropocollagen molecules [35], where it was shown that homogeneous shear is only possible when the overlap length is below the characteristic length and that fracture like slip pulses develop for larger overlapping lengths.

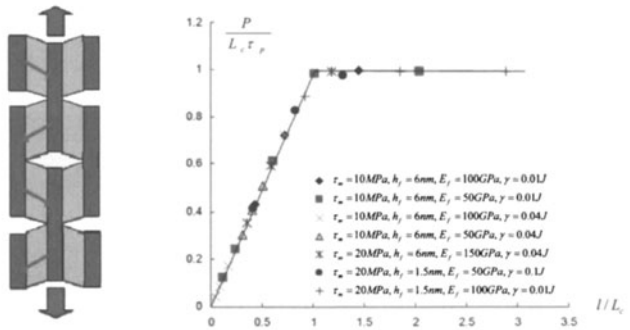

Figure 5. The scaling law of the normalized pulling force as a function of the normalized platelet length for the staggered composite. The simulation results under different combinations of parameters show excellent comparison with the theoretical prediction based on Eq. (4), which is shown as the solid line [30].

The principle of optimal stress transfer in the matrix thus provides a condition to determine the aspect ratio of particles as

$$\rho = \min\left(\frac{S}{\tau_p}, \sqrt{\frac{2E\Theta_p(1-\varphi)}{\varphi \tau_p}}\right) \qquad (6)$$

Principle III: Selection of volume fraction of hard particles for optimal balance between stiffness and toughness

After the characteristic length and aspect ratio of hard particles have been determined to ensure uniform stress of materials up to the failure point in both particles and matrix, the volume fraction of hard particles can be further selected to achieve the desired objective in mechanical properties. For bone, this objective is expected to be a combined stiffness and toughness. The toughness of the structure is expected to rise as the volume fraction of the hard material decreases. That is, the more soft material in the structure, the higher the toughness, although this may occur at the cost of compromising stiffness of the structure. For example, the toughness is expected to be of increasing importance for sea shells, bone and antelope horn, which correlates with their respective mineral contents of 95%, 45% and 35%, respectively. We will discuss shortly that the toughness of a hierarchical material at one level depends on the strength at the lower level, i.e. higher strength at the (n-1)th level results in higher toughness at the nth level. This is a unique property of hierarchical materials.

That bone and bone-like materials have been evolved to achieve a balance between toughness and stiffness should be apparent in their staggered structure. Studies based on genetic algorithms [36,6] have shown that the staggered nanostructure of bone could be interpreted as an evolutionary result with the objective to simultaneously optimize stiffness and toughness. This can be explained by comparing three rudimentary composite structures depicted in Fig. 6. If the objective is to optimize stiffness alone, the expected optimal structure would have the horizontal parallel strip configuration (the Voigt upper bound) shown in Figure 6(a). On the other hand, if the objective is to optimize toughness only, the expected optimal structure would be the vertical strip configuration shown in Figure 6(b) in which the soft matrix undergoes completely uniform deformation for maximum energy dissipation. In comparison with the staggered structure of Figure 6(c), the horizontal strip structure in Figure 6(a) is too brittle as the soft matrix does not have much chance to deform before the hard particles fail; on the other hand, the vertical strip structure in Figure 6(b) is too soft (as soft as the soft phase) and cannot fulfill the structural support function of bone.

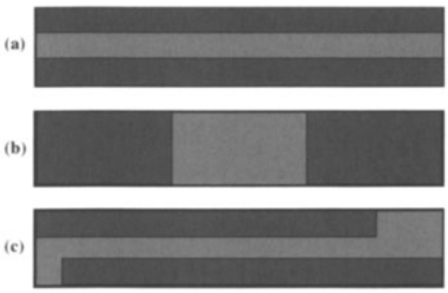

Figure 6. Optimized hard–soft structures with different objective functions. (a) The columnar structure parallel to the direction of loading is expected if the objective is to optimize the stiffness alone. (b) The columnar structure perpendicular to the direction of loading results in uniform deformation in the soft matrix and is expected to be the optimal structure if the objective is to optimize the amount of energy absorption. (c) The staggered structure is expected to be optimal if the objectiveis to optimize both stiffness and toughness of the structure [6].

BOTTOM-UP DESIGN OF SELF-SIMILAR HIERARCHY

We now apply the above principles to assemble a self-similar staggered hierarchical composite structure [6,15]. Consider a total of *N* hierarchical levels. At each level, the hard particles and the soft matrix play essentially the same roles, i.e. the slender particles provide structural rigidity while the soft matrix absorbs and dissipates mechanical energy [6,10,15]. For

the self-similar structure, the same three principles, i.e. flaw tolerance, optimal stress transfer and optimal stiffness and toughness, are applied to each level of hierarchy following a bottom-up route. First, the characteristic size scale of the lowest level of structure is determined. Then the properties at the next higher level are calculated based on the current level of structures, and the characteristic size of the next level is determined by using the criterion of flaw tolerance. This iterative process is repeated until all N levels are determined [6,15].

At the lowest level, the flaw tolerance condition can be readily expressed in terms of the material constants of mineral as

$$\frac{\Gamma_0 E_0}{S_0^2 h_0} = \frac{2\gamma E_m}{\sigma_{th}^2 h_0} = 1, \tag{7}$$

where $E_0 = E_m$ is the Young's modulus of the mineral, γ is the surface energy and σ_{th} is the theoretical strength of mineral. According to Principle I, The characteristic size of the mineral particles is selected as

$$h_0 = \frac{2\gamma E_m}{\sigma_{th}^2}. \tag{8}$$

For bio-minerals, we take $\gamma = 1$ J/m^2, $E_m = 100$ GPa and $\sigma_{th} = E_m / 30$, and find

$h_0 = 18$ nm.

This nanoscale size becomes the basis for designing structures at higher levels of hierarchy. Assuming that the structure of the n-th hierarchical level has been determined, the effective Young's modulus at the (n+1)-th hierarchical level E_{n+1} can be calculated as [6,10,15] as

$$\frac{1}{E_{n+1}} = \frac{4(1-\varphi_n)}{G_n^p \varphi_n^2 \rho_n^2} + \frac{1}{\varphi_n E_n}, \tag{9}$$

where G_n^p is the shear modulus of the soft matrix at the n-th level, and E_n, φ_n, ρ_n are Young's modulus, volume fraction and aspect ratio of the hard particles at the n-th level. Actually, the elastic properties of the hard particles at higher hierarchical levels are anisotropic. For simplicity, here we only consider the effective Young's modulus under uniaxial tension. In comparison, the Voigt upper bound of composite stiffness at the (n+1)-th level is

$$E_{n+1}^{\text{Voigt}} = (1-\varphi_n)E_n^p + \varphi_n E_n \cong \varphi_n E_n,$$

where E_n^p is the Young's modulus of the soft phase at the n-th level. When the total volume fraction of mineral $\Phi = \varphi_0 \varphi_1 \cdots \varphi_{N-1} = \prod_{n=0}^{N-1} \varphi_n$ is fixed, increasing the total number of hierarchy levels N tends to increase φ_n, allowing E_{n+1} of Eq. (9) to approach the Voigt bound E_{n+1}^{Voigt}. Therefore, larger N generally leads to higher overall stiffness of the composite.

When the staggered structure is subjected to uniaxial tension, the mineral particles are primarily under tension with protein layers in-between transfer loads primarily via shear [10]. By means of self-similar design, this feature is carried over to all hierarchical levels. Assuming that the particle aspect ratio is determined by the particle to matrix strength ratio [6,15], the tensile limiting strength at the (n+1)-th level depends on which phase of the n-th level fails first. If the hard particles fail first, we have $S_{n+1} = \varphi_n S_n / 2$. On the other hand, if the soft matrix fails first, in the most efficient way [30] that the stress transfer in the matrix remains uniform [6,10], we will

have $S_{n+1} = \varphi_n \rho_n \tau_n^p / 2$, where τ_n^p stands for the shear strength of the soft matrix. Therefore, the strength of the hard particles at the (n+1)-th level can be expressed as

$$S_{n+1} = \min\left(\frac{\varphi_n \rho_n \tau_n^p}{2}, \frac{\varphi_n S_n}{2} \right). \quad (10)$$

From the energy dissipation point of view, it is important that the soft matrix undergoes large deformation and sliding before the hard particles fail under tension. An optimal design is that the soft matrix should fail simultaneously with the hard particles. Under this condition,

$$\rho_n \tau_n^p = S_n, \quad (11)$$

and the tensile strength of the self-similar bone at the (n+1)-th level is

$$S_{n+1} = \varphi_n S_n / 2, \; S_0 = \sigma_{\text{th}}. \quad (12)$$

For the staggered structure at the (n+1)-th level, the effective fracture energy should include the energy required to break both the hard particles and soft matrix of the n-th level. Therefore, it can be expressed as

$$\Gamma_{n+1} = \varphi_n \Gamma_n + (1-\varphi_n) l_n \tau_n^p \Theta_n^p, \quad (13)$$

where Θ_n^p denotes the effective strain measuring the range of deformation of the soft matrix at the n-th level. On the right-hand side of Eq. (13), the first part stands for the energy required to break the hard particles while the second part refers to the fracture energy corresponding to the soft matrix. Here the width of the fracture process zone is assumed to be on the order of the length of the hard particles l_n. For simplicity, we assume that the strain energy is primarily dissipated by the deformation of the soft matrix at any hierarchical level. Eq. (13) can be reduced to

$$\Gamma_{n+1} \cong (1-\varphi_n) l_n \tau_n^p \Theta_n^p = (1-\varphi_n) h_n S_n \Theta_n^p, \quad (14)$$

where Eq. (11) has been adopted.

Once we have calculated E_{n+1}, S_{n+1} and Γ_{n+1}, the characteristic size of flaw tolerance at the (n+1)-th level can be determined according to Eq. (2) as

$$h_{n+1} = \frac{\Gamma_{n+1} E_{n+1}}{S_{n+1}^2}. \quad (15)$$

Substituting Eqs. (12) and (14) into (15) yields

$$\frac{h_{n+1}}{h_n} = \frac{4(1-\varphi_n)\Theta_n^p E_{n+1}}{\varphi_n^2 S_n}, \quad (16)$$

where E_{n+1} is given by Eq. (9). From Eqs. (8) and (16), the hierarchical structure can thus be determined in the following bottom-up sequence

$$h_0 \to h_1 \to h_2 \to \cdots \to h_N = H,$$

provided that φ_n, Θ_n^p are known.

In order to demonstrate the properties of such hypothetical hierarchical material, we have performed calculations based on some specific parameter choices [6,15]. For simplicity, we assume that the volume fraction φ_n and the aspect ratio ρ_n of each level are identical, i.e., $\rho_n = \rho$, $\varphi_n = \varphi$, so that the structure becomes self-similar and the volume fraction of the hard particles in each level is related to the total fraction Φ of mineral as

$$\varphi = \Phi^{1/N}. \quad (17)$$